

Estimation of Stiffness derivative for Ogives at Constant specific heat Ratio $\gamma = 1.666$ at Hypersonic Mach Numbers

Aysha Shabana^a, Shamitha^b, Asha Crasta^c, and S. A. Khan^d

^aResearch Scholar, Mathematics Dept., M.I.T.E, Moodabidri and Assistant Professor, SCEM, Mangaluru, affiliated to VTU, Karnataka, India

^b Research Scholar, Mathematics Dept., M.I.T.E, Moodabidri, affiliated to VTU Karnataka, India

^cAssociate Professor, Mathematics Department, M.I.T.E, Moodabidri, affiliated to VTU Karnataka, India

^d Professor, Department of Mechanical Engineering, Faculty of Engineering, IIUM, Gombak Campus, Kuala Lumpur, Malaysia.

Article History: Received: 10 January 2021; Revised: 12 February 2021; Accepted: 27 March 2021; Published online: 28 April 2021

Abstract: Specific heat ratios play an essential role in the design of an ogive of an aircraft, which in turn makes it a priority point in estimating the stiffness derivative, keeping in mind the stability of an airplane. One such attempt is made here where the study of stiffness derivative is done for specific heat ratio = 1.666 for other than the air. In some cases, higher values of specific heat ratios become a priority to stimulate the flow. For δ angles from 50 to 300, results have been obtained. For pivot locations near the nose, the pitching moment assumes higher values as compared to the pivot position near the shoulder of the ogive. The stability derivatives attain negative values for $h = 0.6$, and its importance is maximum at $h = 1$.

Keywords:

1. Introduction

The stability derivative assumes a significant part and its criticalness in the exhibition of aerospace vehicles at high Mach numbers. At significantly large inertia level, the nose of aviation vehicles either be with low L/D ratio or obtuse as the aerodynamic heating of the streamlined bodies is of significant concern. The assessment of performance in the pitch mode of the for the missiles, the stiffness derivatives is of significance, and inspection for symmetric pivot ogives at a large stream is introduced here. The current study is for the case, while the shock wave is close for an ogive with a strident nose that can be utilized in the forthcoming to progressively helpful models joining the factor because of gruffness. This study further gains importance due to the change of the working medium. Usually, researchers consider air as the working medium and obtain the results for stability derivatives. However, there are cases when the working medium need not be air but some other medium like helium, argon, and Co₂, etc. This paper focuses attention on estimating the stability derivatives for a medium other than the air. The specific heat ratio for air is $\gamma = 1.4$ is valid for a perfect gas. It is observed in the literature that the gas can be either thermally ideal or calorically ideal gas. For a calorically ideal gas, the γ of the gas at constant pressure and volume is not a function of temperature. However, for a thermally ideal gas, even though the specific heat ratio is a function of temperature but still when we estimate the specific heat ratio when pressure and volume are constant, its value stay on 1.4. While inspecting the literature, it found that up to a temperature of 800 K, the air can be assumed to be a perfect gas. But in view of the growth in the inertia, the temperature will further increase. As per the kinetic theory of gases, when due to the increase in Mach values, the temperature is further increased to 2000 K, the oxygen which is non-reacting flow will be ionized, and with a further rise in the Mach values, the temperature will rise. At a temperature of 4000 K, the nitrogen will also become ionized. Hence, at a temperature around 4000 K, the air is fully ionized and becomes a reacting flow. This study was undertaken to look for some other alternative gas as the medium for the stream to account for this issue of aerodynamic heating at high Mach numbers. The literature review suggests that we can simulate the high-speed flow by assuming a specific heat ratio as two, whereas for air, it is 1.4. Conducting experiments in a water tunnel are cost-effective and yet gives good results. Hence, the present suggested by the present theory gives reasonably good results with computational ease.

The hypothesis of likeness for the hypersonic stream, which is substantial on the compression side of the airfoil with an extreme pitch rate, was created by Ghosh [1]. However, he stated that Mach just behind the shockwave is more significant and more than 2.5 with an appended curved shock. The expansion of Ghosh's research for wedges without planar shape due to the rate of change in pitch motion was extended by Crasta and Khan to assess the streamlined permanence results in a pitch for together at $M \leq 5$ [2] and $M > 5$ streams [10] to [12].

Ghosh K. [2] broadened his hypothesis of a high angle of attack [1] for bodies of revolution, understanding the proportionality of movement in a cylinder with pivotal evenness, that is free of 1-D fluid flow [1], which brings

about a comparable conical-annular region. Ghosh, K., [2] demonstrates that a cylinder movement in the conical-annular territory. Ghosh, K., [2] gives a hypersonic semblance based answer in case of a cone, that shapes the key for a viscous boundary layer of secure thickness. Outcomes are created for the high Mach and for a thermally ideal gas for ogives in pitch for different inactivity levels and stream diversion points.

2. Analysis

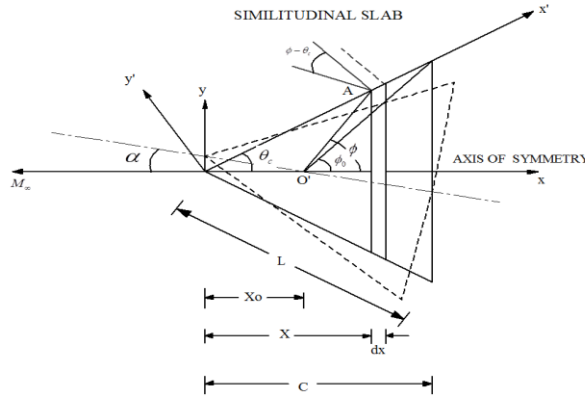


Figure 1: Geometry of the cone

Figure 1 shows the geometry used for this study.

$$\tan \phi = \frac{x \tan \theta_c}{(x - x_0)} ; \tan \phi_0 = \frac{c \tan \theta_c}{(c - x_0)}$$

The slant made by A at O through x-axis is phi, and at the numerous location of A, phi changes in the range from pi to phi_c,

The angle of the ogive theta_c with c

The pitching derivative for stiffness is obtainable by C_m_alpha

$$C_{m_\alpha} = \left[\frac{\partial M}{\partial \alpha} \right]_{\alpha, q \rightarrow 0} \frac{1}{\frac{1}{2} P_\infty U_\infty^2 S_b c}$$

$$S_b = \text{ogive surface area} = \pi (c \tan \theta_c)^2,$$

Solving and simplifying we arrive at,

The relations for P2/P1 is the pressure ratio for a cone when the angle of attack is zero under the steady condition (Ghosh, K., 1984), given that shock, is affixed at the tip of the front point of the body is

$$\frac{P_{bo}}{P_\infty} = 1 + \gamma M_{po}^2 \left(1 + \frac{1}{4} \varepsilon \right) \tag{1}$$

Here epsilon is the mass per unit volume (i.e., density ratio)

$$\varepsilon = \frac{2 + (\gamma - 1) M_{po}^2}{2 + (\gamma + 1) M_{po}^2} \tag{2}$$

Where M_po is the temporal inertia level at the piston, that runs in a conical-annular, P_bo is compression side pressure on the surface of the aerodynamic body when the incidence angle is zero

$$M_{po} = M_\infty \sin \theta_c$$

and

$$\frac{dP_{bo}}{dM_{po}} = 2\gamma P_{\infty} M_{po} \left[1 + \frac{1}{4} \left(\varepsilon + \frac{1}{2} M_{po} \cdot \frac{d\varepsilon}{dM_{po}} \right) \right] \quad (3)$$

Where

$$\frac{d\varepsilon}{dM_{po}} = \frac{-8M_{po}}{N^2} + \lambda' f \left\{ \frac{8K(3(\gamma+1)K^2 - 2)}{N^3} \right\} \quad (4)$$

And $N = [2 + (\gamma + 1)M_{po}^2]$

On resolving (3), we have

$$\frac{dP_{bo}}{dM_{po}} = 2\gamma P_{\infty} M_{po} \left[(a_1 + \lambda' a_2) - \frac{2a_2 \lambda' h \tan \phi}{\tan \phi - \tan \theta_c} \right] \quad (5)$$

$$h = \frac{x_0}{c},$$

$$\lambda' = \frac{\lambda}{\tan \theta_c}, \quad a_1 = 1 + \frac{\varepsilon}{4} - \frac{K^2}{N^2}, \text{ and } a_2 = 1 + \frac{\varepsilon}{4} - \frac{K^2(N+8)}{N^3}$$

The resulting analytical equations are used to estimate the results in a pitch for the stability of a pitching cone at numerous angles of attack and Mach numbers.

$$C_{m_{\alpha}} = [C_{m_{\alpha}}]_{cone} + \frac{2\lambda' a_2}{3(1+n^2)} \left[h^3 \{1 - 2n^2 - h(1 - 3n^2)\} + (1-h) \{H(1+h+h^2) + 3n^2 h^3\} \right]$$

Everywhere

$$[C_{m_{\alpha}}]_{cone} = D \left[h^3 (1 - 2n^2) - (1-h) \{H(2+h) + n^2 h(1+2h)\} \right]$$

$$D = \frac{2}{3(1+n^2)} \left[1 + \frac{1}{4} \left(\varepsilon + \frac{1}{2} K \frac{d\varepsilon}{dM_{po}} \right) \right] \quad (7)$$

$$H = (1 - h + n^2)$$

And $n = \tan \theta_c$

Based on the over-analysis, the results were obtained for a broad stretch of Mach values and incidence angles.

3.Results and Discussion:

This analysis was performed to calculate the rigidity offshoots in pitch for cones and ogives for numerous angles of prevalence and the Mach values. In the present study, the working medium considered is other than air.

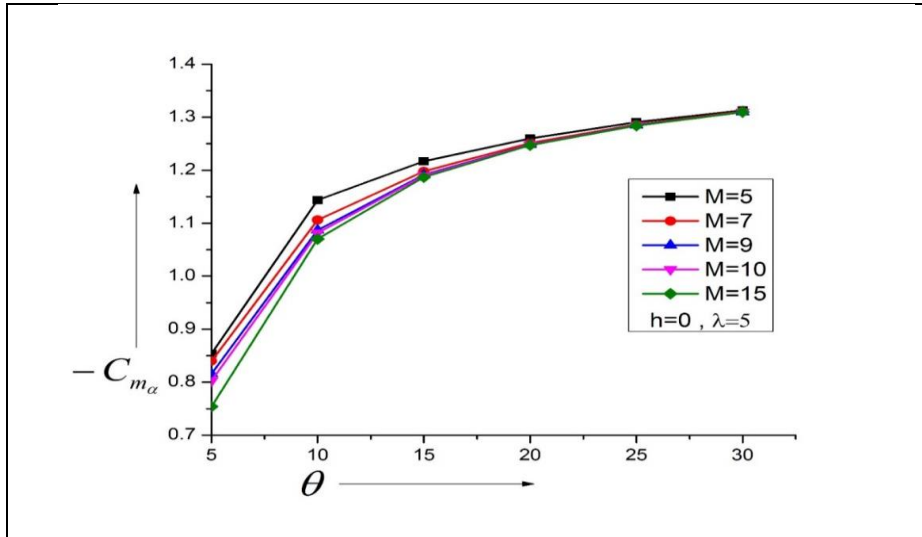


Fig. 2 $C_{m\alpha}$ Vs. θ , and $h = 0$

This segment deliberates the outcomes of rigidity derived from ogive. To accomplish ogive, we considered the original state of the cone, and afterward, a circular section has been overlaid to achieve the ideal Ogival shape. For a presented estimation of λ , the angle (θ) of the cone ranging from 5° to 30° , and the Mach Number varied from 5 to 15, keeping other variables the same. Figs. 2 to 7 represent the outcomes in the case of $\lambda = 5$. Fig. 2 shows the results for $h = 0$ and $\lambda = 5$, for (θ) in the range from 5° to 30° and Mach Number 5 to 15. From the results of figure 2, it is found there is a consistent increment in the rigidity derivatives.

The physical science at the back of this trend in the Stiffness derivatives is because of the change in the wetted area of the ogive. Aimed at a static angle of 5° , the stiffness derivative increases by 1.65 %, 2.88 %, 1.56%, and 6 % for Mach Number varying from 5 to 7, 7 to 9, 9 to 10 and 10 to 15 respectively. For constant value of Mach 5, the stiffness derivative increases by 25 %, 6%, 3.4 %, 2.36 % and 1.72% for angle δ varying since 5 to 10, 10 to 15, 15 to 20, 20 to 25 and 25 to 30 respectively. The variation in the stiffness derivatives is non-linear. The shape of the ogive and the pressure distribution at various flow deflection angle and Mach number may be possible reasons for this behavior.

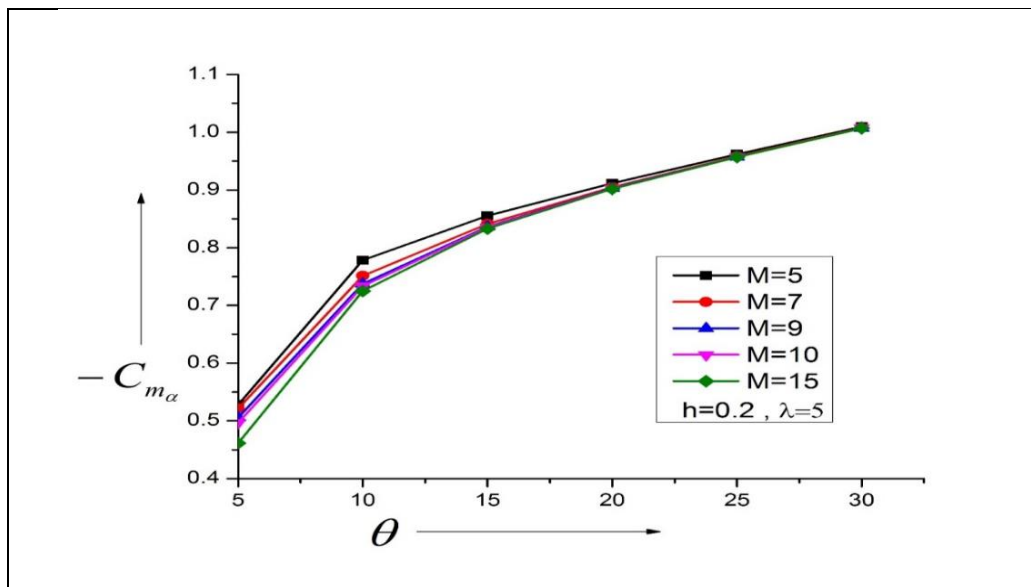


Fig. 3 $C_{m\alpha}$ Vs. θ , and $h = 0.2$

The outcome for $h = 0.2$ is produced in Fig. 3, retaining the remainder of the factors the same. However, the pivot position is changed and shifted in the direction of the shoulder of the ogive. Here we consider the stiffness offshoots for $h = 0.2$. From figure 3, they show a similar pattern when we compare the results with Fig. 2, except the magnitude is decreased due to the shift in the axis point. This trend will continue as we are moving towards

the trailing edge. For a static amount of angle δ of 5° , the stiffness derivative increases by 1.24 %, 3 %, 1.75%, and 7% for Mach Number varying from 5 to 7, 7 to 9, 9 to 10, and 10 to 15 respectively. For a constant value of Mach $M = 5$, the stiffness derivative increases by 32 %, 8.98%, 6.15 %, 5.2 % and 4.74% for angle δ varying from 5° to 10° , 10° to 15° , 15° to 20° , 20° to 25° and 25° to 30° respectively.

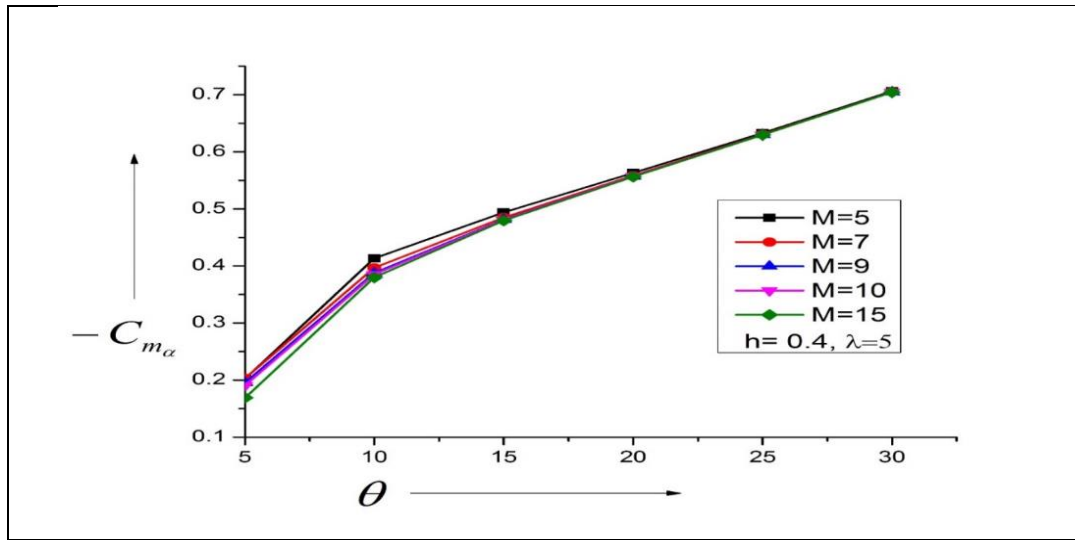


Fig. 4 $C_{m\alpha}$ Vs. θ , and $h = 0.4$

The outcome for the hinge stance $h = 0.4$ is shown in Fig. 4 retaining every previous parameter equivalent. The results for $h = 0.4$ show similar trends with the exemption that the magnitude has decreased significantly owing to the reduction at the moment as the pivot has additionally transferred in the direction of the straggling edge. For a constant estimation of angle of 5° , the rigidity derivative increases by 0.45 %, 3.65%, 2.54%, and 11.48% for Mach Number shifting from 5 to 7, 7 to 9, 9 to 10 and 10 to 15 individually. For a fixed estimation of Mach number 5, the stiffness derivative increments by 51 %, 16.33%, 12.27 %, 11 % and 10.38 % for semi vertex edge shifting from 5 to 10, 10 to 15, 15 to 20, 20 to 25 and 25 to 30 separately.

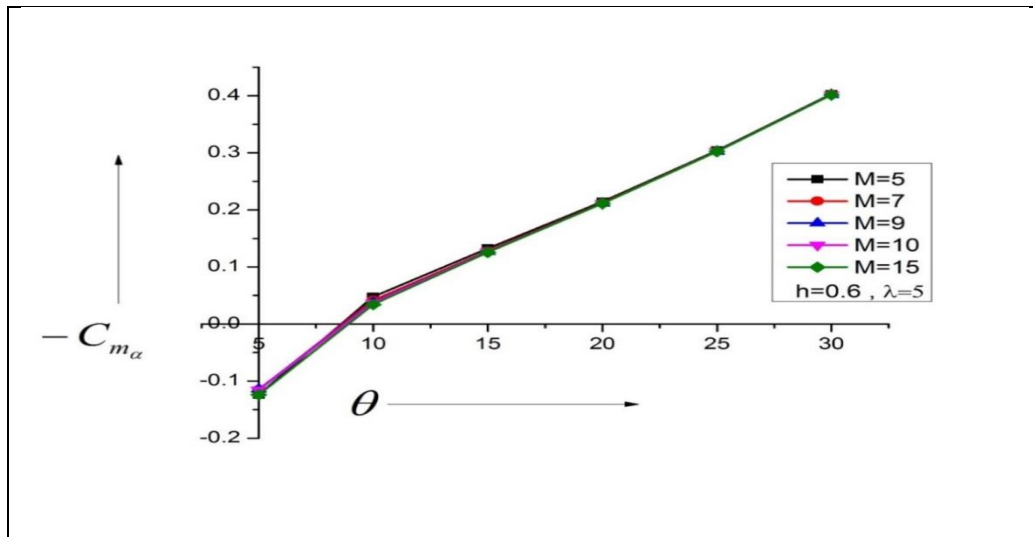


Fig. 5 Fig. 2 $C_{m\alpha}$ Vs. θ , and $h = 0.6$

For the fulcrum stance of $h = 0.6$, the outcome of rigidity derivatives is exhibited in Fig. 5. It is seen that the results show a different trend. This may be due to the selection of the pivot position, which happens to be in the neighborhood of where the normal force is situated at axis of evenness of the cone. Initially, up to angles δ of ten degrees, the sign of the stability derivative is negative. For a higher flow deflection angle, it assumes normal values as expected. For a fixed estimation of Mach number 5, the stiffness derivative increments by 75.8 %, 63.8%, 38.24 %, 29.5 % and 24.49 % for semi vertex angle varying from 5 to 10, 10 to 15, 15 to 20, 20 to 25 and 25 to 30 separately.

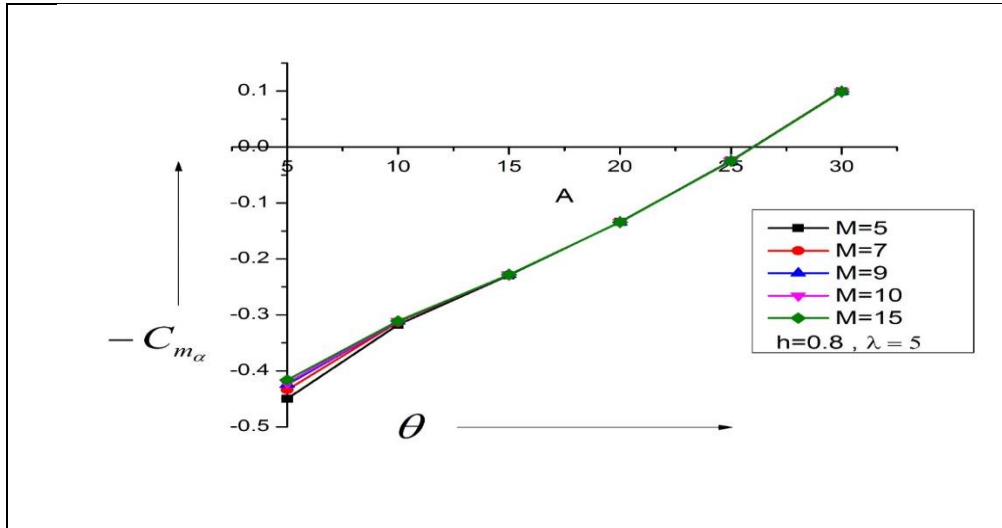


Fig.6 C_{m_α} Vs. θ , and $h = 0.8$

The toughness derivatives outcomes are exhibited in Fig. 6 for hinge point $h = 0.8$. Since the choice of the pivot position is following the location of the normal force, it scores in negative values of the static margin. However, we see the increment in the rigidity derivative in conjunction with the rise in the angle δ . But the influence of the Mach M is negligible. For a static quantity of angle δ of five degrees, the stiffness derivative increases by 3.55 %, 2.17 %, 0.67%, and 1.22% for Mach Number varying from 5 to 7, 7 to 9, 9 to 10 and 10 to 15 respectively. For a fixed estimation of Mach number 5, the stiffness derivative increases by 29.4 %, 27.81%, 41.43 %, 81.6 % and 124.84% for angle δ varying from 5 to 10, 10 to 15, 15 to 20, 20 to 25 and 25 to 30 respectively.

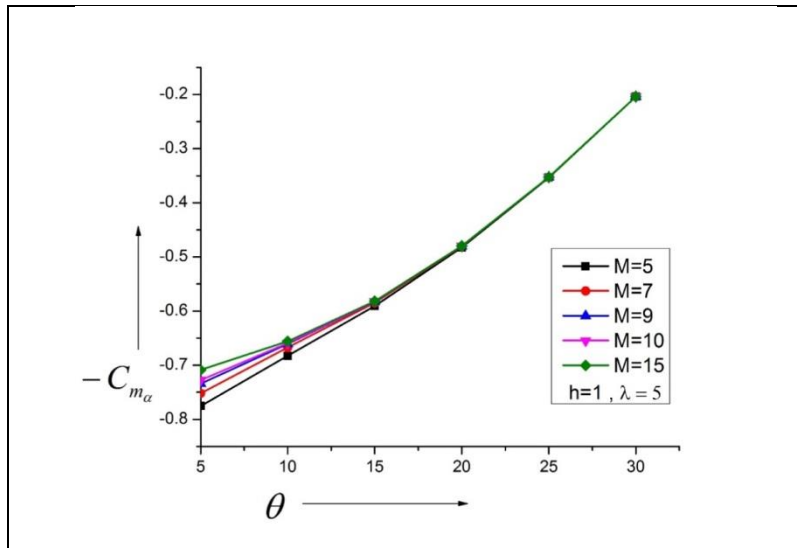


Fig.7 Fig. 2 C_{m_α} Vs. θ , and $h = 1$

Findings for the swivel point of $h = 1$ are presented in Fig. 7, preserving every other constraint the similar. Since this location is at the shoulder of the ogive, this location of the pivot position will affect in a considerable moment arm, and the position of the lift force is ahead of the pivot position. Results indicate that the magnitude remained negative, resulting in a negative static margin.

Intended constant magnitude of angle δ of 5° , the stiffness derivative increments by 3 %, 2.37 %, 0.92% and 2.57 % for Mach Number changing from 5 to 7, 7 to 9, 9 to 10 and 10 to 15 respectively. For a constant value of Mach $M = 5$, the stiffness derivative increases by 11.96 %, 13.49%, 18.26 %, 26.77 % and 42.26% for angle δ varying from 5 to 10, 10 to 15, 15 to 20, 20 to 25 and 25 to 30 respectively.

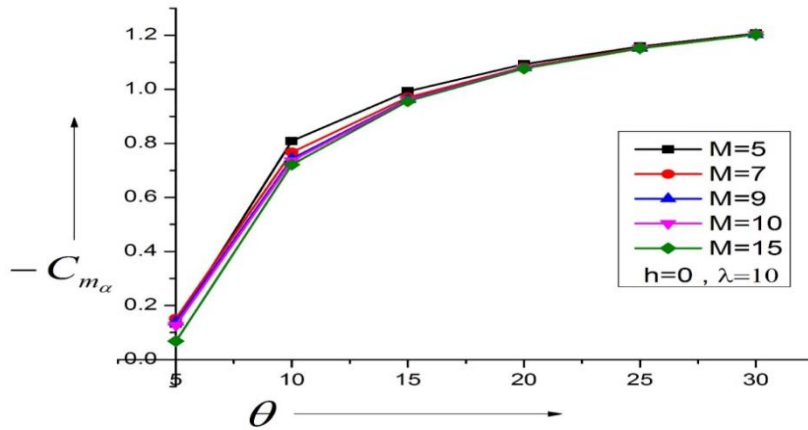


Fig. 8 $C_{m\alpha}$ Vs. θ , and $h = 0$

Findings for $\lambda = 10$ are introduced in Figs. 8 to 13. Findings for $h = 0$ and $\lambda = 10$ is demonstrated in Fig. 8, for the angle (θ) in the stretch from 5 to 30 degrees and Mach Number 5 to 15.

It is found that there is a ceaseless increment in the rigidity derivative along with the rise in angle δ for the whole range of Mach numbers. The physical explanation behind the addition in the Stiffness derivative is because of the increased surface area of the ogive. For a static estimation of angle δ of five degrees, the stiffness derivative increases by 12.74 %, 8.05 %, 8.46%, and 46.6 % for Mach Number fluctuating from 5 to 7, 7 to 9, 9 to 10 and 10 to 15 respectively. For a permanent value of Mach $M = 5$, the stiffness derivative increases by 83.63 % , 18.55%, 9.14 % , 5.71 % and 3.93% for angle δ shifting since 5 to 10, 10 to 15, 15 to 20, 20 to 25 and 25 to 30 respectively. Here is a significant growth in the rigidity derivatives, and after a certain value of the angle δ , the growth in the stability derivative is not seen as it has achieved the optimum values. Also, as the Mach number increases after a certain Mach number, the increase is minimal. This trend may be attributed due to the change in the intensity of the shock wave at various Mach numbers and the pressure on the nose portion of the cone. Hence, it can be attributed due to the combined defect of the inertia level, flow deflection angle, and the cone/ogive surface pressure

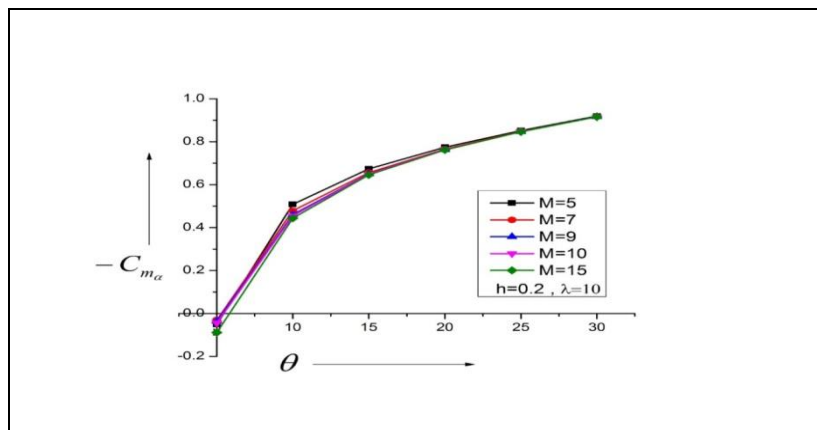


Fig. 9 $C_{m\alpha}$ Vs. θ , and $h = 0.2$

Stiffness derivative plot for pivot $h = 0.2$ is shown in Fig. 9, for diverse Mach M and flow angles. The figure indicates that these results are different from those of when $\lambda = 5$. Due to enhanced values of the λ has modified the surface pressure on the nose ogive. It shows a reversal in the trends. From the stability aspect, it is a very significant change in the stability derivative. As a designer, one needs to keep this aspect of the ogival shape in mind as this will lead to instability in the aerospace vehicles.

Intended for a permanent estimation of angle δ of five degrees, the stiffness derivative increases by 40.15 %, 17 %, 18.2% and 49.7% for Mach Number fluctuating from 5 to 7, 7 to 9, 9 to 10 and 10 to 15 separately. For a fixed estimation of Mach number 5, the stiffness derivative increments by 109.9 % , 24.48%, 13 % , 9.15 % and 7.31% for angle δ varying since 5 to 10, 10 to 15, 15 to 20, 20 to 25 and 25 to 30 separately

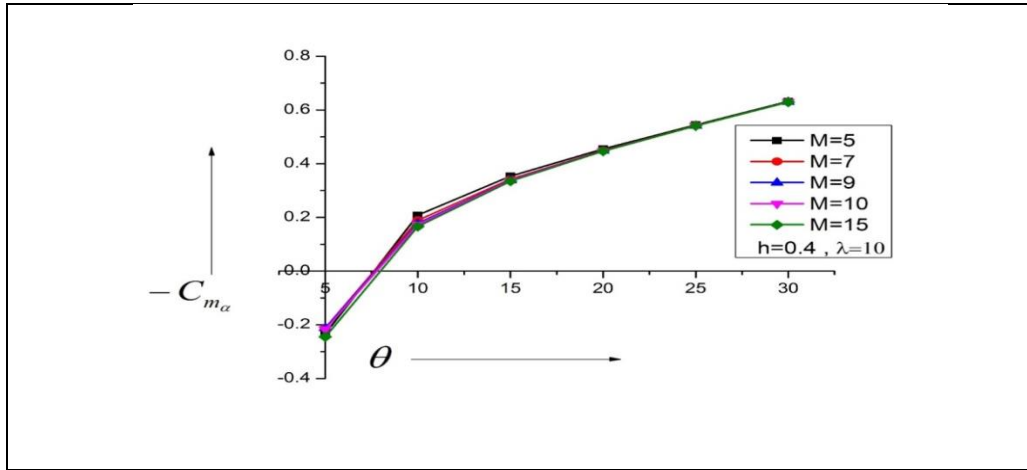


Fig. 10 $C_{m\alpha}$ Vs. θ , and $h = 0.4$

For pitching place, $h = 0.4$, the rigidity derivatives findings are demonstrated in Fig. 10. Because of the alteration in the swing position towards the trailing edge, there is further variation in the rigidity derivatives. For a static estimation of angle δ of 5° , the stiffness derivative increments by 9 %, 0.08 %, 2%, and 11.54% for Mach Number shifting from 5 to 7, 7 to 9, 9 to 10, and 10 to 15 respectively. For a constant value of Mach $M = 5$, the stiffness derivative increments by 189.3%, 41.14%, 22.26 %, 16.49 % and 13.76% for angle δ differing from 5 to 10, 10 to 15, 15 to 20, 20 to 25 and 25 to 30 individually

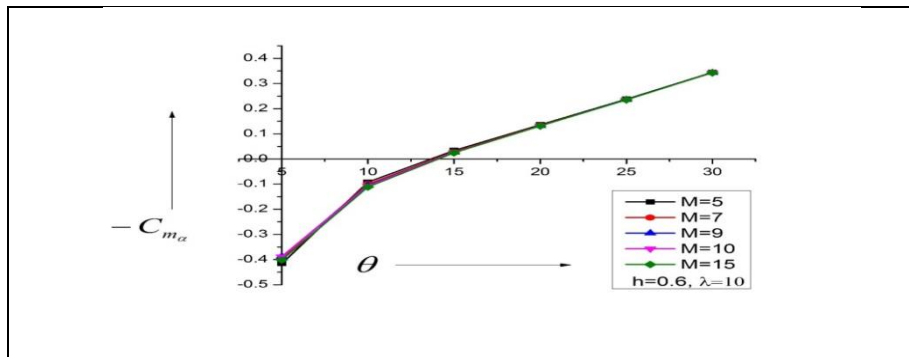


Fig.11 $C_{m\alpha}$ Vs. θ , and $h = 0.6$

For swing place, $h = 0.6$. The toughness results scores are exhibited in figure 11. This position is very closed to the location where the lift force is located and hence will lead to lower static margins. For his case, the Mach number has no role to play. Even though the Mach M is grown from 5 to 15, it does not yield any significant change over in the rigidity derivatives. For a static estimation of angle δ of five degrees, the stiffness derivative increments by 5.28%, 1.48 %, 0.18% and 3.14% for Mach Number fluctuating from 5 to 7, 7 to 9, 9 to 10 and 10 to 15 respectively. For a fixed estimation of Mach number 5, the stiffness derivative increments by 77.82%, 136.72%, 75 %, 42.8 % and 31% for semi vertex angle differing from 5 to 10, 10 to 15, 15 to 20, 20 to 25 and 25 to 30 individually.

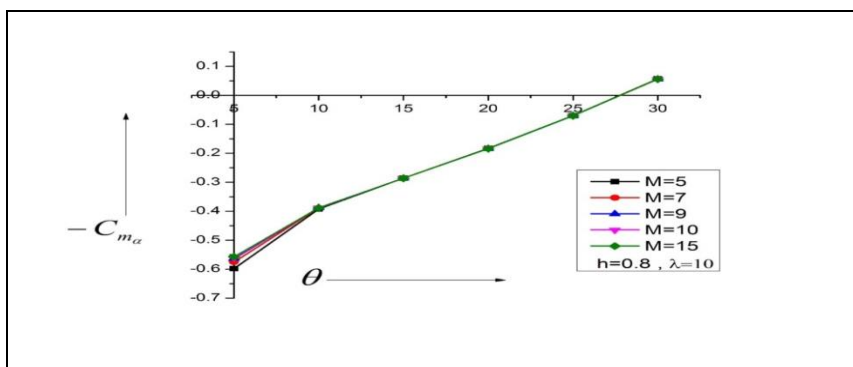


Fig.12 $C_{m\alpha}$ Vs. θ , and $h = 0.8$

The rigidity derivatives findings are depicted in Fig.12 for hinge position $h = 0.8$. The outcomes are astonishing, as the estimations of stiffness derivatives are in the negative since the position of the hinge position is

following the location of the center of pressure resulting in pitch up moment and hence a negative static Margin. However, we see a rise in the rigidity derivative with the growth in the angle δ for the entire range of the Mach numbers of the current research. As discussed above, the Mach number has a marginal effect on the stability derivatives. This may be owing to the growth in the outside zone. For a static estimation of angle δ of five degrees, the stiffness derivative increases by 3.82 %, 2 %, 0.54% and 0.54% for Mach Number differing from 5 to 7, 7 to 9, 9 to 10 and 10 to 15 individually. For a fixed estimation of Mach number 5, the stiffness derivative increments by 34.4 %, 27.16%, 35.9 %, 61.9 % and 181.38% for semi vertex angle shifting from 5 to 10, 10 to 15, 15 to 20, 20 to 25 and 25 to 30 respectively.

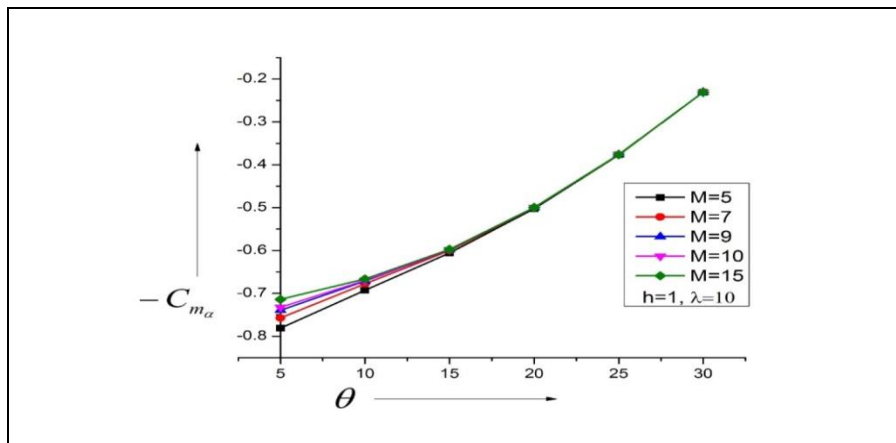


Fig.13 $C_{m\alpha}$ Vs. θ , and $h = 1$

Findings for hinge posture of $h = 1$ are depicted in Fig. 13. This pivot position is at the extreme position of the ogive and located at the end of the nose length. Mach number has no influence on the stability derivatives except at lesser tenets of angle δ . For a static estimation of angle δ of 5° , the stiffness derivative increments by 3 %, 2.36%, 0.91%, and 2.54 % for Mach Number differing from 5 to 7, 7 to 9, 9 to 10, and 10 to 15 respectively. For a fixed estimation of Mach number 5, the stiffness derivative increments by 11.29%, 12.58%, 17 %, 24.94 % and 38.8% for semi vertex angle shifts from 5 to 10, 10 to 15, 15 to 20, 20 to 25 and 25 to 30 respectively.

Conclusion

In view of the above discussion, the results may be summarized as under:

1. For lower Mach number, there is a strong dependence of the stiffness derivatives on Mach M as well as the angles δ .
2. At the trailing edge or the shoulder of the ogive, the stability derivative is harmful and results in pitch up moment, which is undesirable from the steadiness viewpoint.
3. For lower values of λ , there is a strong dependence of stiffness derivative on the pivot position.
4. For large values of λ , there is a change in the behavior of the stability derivatives.
5. This may be due to the difference in the surface pressure of the ogive. And hence the location of the lift force, that ends in a negative moment.
6. When the location of the pitching point is shifted downstream leads to lower values of the stability derivatives.
7. For large values of λ , there is a change in the behavior of pitching moment, and it becomes autonomous of Mach M .

The effect of the incidence angle continues to result in higher values of the pitching moment.

References

1. Ghosh, K., 1977. A New Similitude for Aerofoils in Hypersonic Flow. Proceedings of the 6th Canadian Congress of Applied Mechanics, Vancouver, Canada, May 29-June 3, pp. 685-686.
2. Ghosh, K., 1984. Hypersonic large deflection similitude for oscillating delta wings. The Aeronautical Journal, pp. 357-361.
3. Khan, S. A., and Asha Crasta, 2010. Oscillating Supersonic delta wings with curved leading Edges. Advanced Studies in Contemporary Mathematics, 20(3), pp. 359-372.
4. Asha Crasta and S. A. Khan, 2013. Effect of Angle of Incidence on Stability derivatives of a Wing, IET Conference Publications
5. Asha Crasta, S. A. Khan, 2013 Determination of Surface Pressure of an axisymmetric ogive in Hypersonic Flow. Mathematical Sciences International Research Journal, Vol. 2, Issue 2, August 2013, pp.333-335, ISSN: 2278-8697.
6. Asha Crasta and S. A. Khan, 2015. Effect of Angle of the attack on Stiffness derivative of an oscillating supersonic delta wing with curved leading edges. IOSR-JMCE, issue 1, Volume 12, December, pp 12-25.

7. Asha Crasta and S. A. Khan, 2015. Effect of Angle of the attack on Damping derivative of a delta wing with full sine curved leading edges. IJETED Journal issue 5, Volume 1, December- January.
8. Asha Crasta and S. A. Khan, 2015. Estimation of Damping derivative of a delta wing with half-sine curved leading edges. IOSR Journal of Mechanical and civil engineering, Vol. 12, issue 1, February, pp 40-44.
9. Asha Crasta and S. A. Khan ,2015. Estimation of Damping derivative in the pitch of a Supersonic delta wing with curved leading edges. IOSR Journal of Journal of Mathematics, Vol. 1, issue 1, Jan-Feb, pp.07-15.
10. Asha Crasta, Pavitra S, S.A. Khan 2016," Estimation Of Surface Pressure Distribution On A Delta Wing With Curved Leading Edges In Hypersonic/Supersonic Flow," International journal of energy, environment, and Economics, Nova Science publishers inc, Vol 24, pp.67-73.
11. Aysha Shabana, Renita Sharon Monis, Asha Crasta, and S. A. Khan, 2017. Estimation of stability Derivative Of an Oscillating cone in Hypersonic Flow. International Journal of Recent Research Aspects ISSN: 2349-7688, Vol. 4, Issue 4, Dec2017, pp. 46-52.
12. Renita Sharon Monis, Aysha Shabana, Asha Crasta, and S. A. Khan ,2017. Computation of Stiffness Derivative for an unsteady delta wing with curved leading edges. International Journal of Recent Research Aspects ISSN: 2349-7688, Vol. 4, Issue 4, Dec 2017, pp. 69-72.
13. Aysha Shabana, Renita Monis, Asha Crasta S. A. Khan, 2018" Computation of stability derivatives of an oscillating cone for specific heat ratio =1.66," IOP Conf. Series: Materials Science and Engineering 370 (2018) 012059 DOI:10.1088/1757-899X/370/1/012059
14. Aysha Shabana, Renita Monis, Asha Crasta S. A. Khan, 2018" Estimation of stability derivatives in Newtonian Limit for an oscillating cone" IOP Conf. Series: Materials Science and Engineering 370 (2018) 012061 DOI:10.1088/1757-899X/370/1/012061
15. Ayesha Shabana, Renita Sharon Monis, Asha Crasta, and S. A. Khan,2018 "The Computation of Stiffness Derivative for an Ogive in Hypersonic Flow", International Journal of Mechanical and Production Engineering Research and Development (IJMPERED), Vol. 8, Issue 5, pp. 173-184, June, ISSN (online): 2249-8001, ISSN (Print): 2249-6890.
16. Renita Sharon Monis, Aysha Shabana, Asha Crasta, and S. A. Khan, 2019," An Effect of sweep angle on roll Damping derivative for a Delta Wing with curved leading edges in unsteady flow", International Journal of Mechanical and Production Engineering Research and Development (IJMPERED), Vol. 9, Issue 2, pp. 361-374, April, ISSN (online): 2249-8001, ISSN (Print): 2249-6890.
17. Renita Sharon Monis, Aysha Shabana, Asha Crasta, and S. A. Khan, 2019 "Effect of Sweep Angle and a Half Sine Wave on Roll Damping Derivative of a Delta Wing" International Journal of Recent Technology and Engineering (IJRTE) ISSN: 2277-3878, Volume-8, Issue-2S3, pp. 984-989, August, DOI : 10.35940/ijrte.B1184.0782S319
18. Khan, S. A., Aabid, A., & C, A. S. (2019). CFD Simulation with Analytical and Theoretical Validation of Different Flow Parameters for the Wedge at Supersonic Mach Number. International Journal of Mechanical & Mechatronics Engineering IJMME-IJENS, 19(01), 170–177.
19. Khan, S. A., Aabid, A., Mokashi, I., Al-Robaian, A. A., & Alsagri, A. S. (2019a). Optimization of Two-dimensional Wedge Flow Field at Supersonic Mach Number. CFD Letters, 11(5), 80–97.
20. Asrar, W., Baig, M. F., Khan, S. A., "Chaos in WAF projectile motion TX wraparound fins, 34th Aerospace Sciences Meeting and Exhibit, 1996
21. Waqar Asrar, Faisal Mirza Baig, Sher Afghan Khan, "Chaos in Wraparound Fin Projectile Motion," Journal of Guidance Control and Dynamics 21(2):354-356, March 1998, DOI: 10.2514/2.7607
22. Bashir, M., Udayagiri, L., Khan, S. A., Noor, A., "Dynamic stability of unguided projectile with 6-DOF trajectory modeling," 2nd International Conference for Convergence in Technology, I2CT 2017, 2017-January, pp. 1002-1009.
23. Aysha Shabana, Renita Monis, Asha Crasta S. A. Khan, 2018,"Estimation of Stiffness Derivative of an Ogive for Specific Heat Ratio 1.666." TEST Engineering and Management" November-December 2019, ISSN: 0193-4120, Page No. 5091 – 5100